Hyperferroelectricity in ZnO: Evidence from analytic formulation and numerical calculations

Rajendra Adhikari[1,2] and Huaxiang Fu[1]
[1]*Department of Physics, University of Arkansas, Fayettville, Arkansas 72701, USA*
[2]*Department of Natural Sciences, Kathmandu University, Dhulikhel, Kavre, Nepal*

(Received 5 November 2018; revised manuscript received 28 January 2019; published 4 March 2019)

Hyperferroelectricity is an interesting phenomenon. The hexagonal ABC-type semiconductor LiZnAs was discovered to be hyperferroelectric (HFE) [Garrity *et al.*, Phys. Rev. Lett. **112**, 127601 (2014)]. ZnO is a technologically important semiconductor and possesses a wurtzite crystal structure similar to LiZnAs. It raises an intriguing question of whether ZnO is HFE. Here we use various approaches to address this important question by determining the electric equation of state, the free energy of ZnO under an open-circuit boundary condition (OCBC), and the vibration properties of a LO phonon. We find the following: (i) The $D \sim \lambda$ curve of ZnO, where D is electric displacement and $\lambda = P/0.844$ is a parameter directly proportional to polarization P, exhibits one and only one root at $\lambda = 0$. (ii) Under OCBC, the free energy of ZnO does not produce a minimum at the structural phase of nonzero polarization. (iii) The LO phonon with computed frequency $\omega_{\mathrm{LO}} = 255\,\mathrm{cm}^{-1}$ in centrosymmetric ZnO is not soft and does not have an imaginary frequency. These results corroborate the others and consistently lead to the conclusion that, although ZnO is interestingly on the edge of becoming a HFE, it is not yet a HFE. We further provide a physical origin explaining why ZnO is not HFE and reveal a possibility that may turn ZnO into a HFE.

DOI: 10.1103/PhysRevB.99.104101

I. INTRODUCTION

Hyperferroelectricity, in which a *proper* ferroelectric solid of spontaneous polarization maintains its ferroelectricity under an open-circuit boundary condition (OCBC), is an interesting phenomenon of fundamental and technological relevance [1,2]. Fundamentally, unlike in improper ferroelectrics [3–6], the open-circuit boundary condition often generates a strong depolarization field in proper ferroelectrics, which tends to eliminate utterly the ferroelectricity and polarization [7,8]. It is therefore profoundly interesting to understand the physics behind hyperferroelectricity and to investigate why ferroelectricity and atomic off-center displacements persist in hyperferroelectrics (HFE), defying the existence of strong depolarization fields. Possible explanations thus far include small LO/TO splitting [1], competition between well depth and spontaneous polarization [9], instability driven by short-range interaction [10], and metascreening [11]. Furthermore, determination of the free energy when a HFE is under OCBC and determination of the electric equation of state for a HFE are topics of fundamental importance. This knowledge may also help in the future search and design of new hyperferroelectric solids. Technologically, HFE can be used to form interfaces with other functional materials such as semiconductors, topological insulators, and ferromagnetics, where a nonzero polarization maintained in HFE can effectively tune, control, and enhance the properties of the functional materials. Furthermore, certain hyperferroelectrics were shown to have negative longitudinal piezoelectric coefficients [12]. To take advantage of the unusual properties of hyperferroelectricity, determining and understanding whether a solid is HFE are the key.

HFE was discovered recently in hexagonal ABC-type semiconductors such as LiBeSb and LiZnAs [1]. LiZnAs (and LiBeSb) has a crystal structure similar to wurtzite semiconductors, in the sense that Zn and As occupy the atomic sites of the wurtzite lattice. Furthermore, both Zn and As atoms form tetrahedral bonds with their neighbors. The minor difference in LiZnAs compared to the wurtzite structure is the existence of stuffing Li atoms which are located between the atomic layers in the wurtzite structure. Based on the marked resemblance between ABC-type and wurtzite semiconductors, it is intriguing to determine whether the wurtzite semiconductor ZnO is a HFE and to investigate the underlying physics and mechanism behind the conclusion.

ZnO is a polar semiconductor of technological importance [13]. Being polar, ZnO offers an interesting possibility of utilizing its polarization to control the already appealing electronic properties, forming so-called polarization electronics. Also, ZnO has an exceptionally large exciton binding energy of ∼60 meV, suitable for fabricating microelectronics and optical devices that may operate at high temperatures under extreme environments [14]. Meanwhile, ZnO exhibits a large piezoelectric coefficient [15], which makes it an excellent candidate for a piezoelectric semiconductor. ZnO also possesses the largest electromechanical d_{33} coefficient among the wurtzite semiconductors [16], and its $d_{33} = 12.4$ pC/N value is much larger than the $d_{33} = 1.58$ pC/N value in GaN [17]. The large d_{33} coefficient in ZnO originates from the local-polarization rotation mechanism [16], similar to what occurs in ferroelectric solids [18–20]. Moreover, after doping, ZnO shows high electrical conductivity and serves as a good transparent conductor [21–23].

The purpose of this paper is to formulate and use various approaches to determine whether ZnO is HFE and to reveal important physics related to what characteristic properties a HFE should have. The various approaches include (i) the

determination of the electric equation of state, which yields the relationship between electric displacement $\vec{D}$ and polarization $\vec{P}$; (ii) the determination of free energy under the OCBC with a vanishing electric displacement ($\vec{D}=0$); and (iii) the calculation of a longitudinal optic phonon, which reveals lattice stability under the open-circuit boundary condition. These formulated methods are rather general and can be applied to solids other than ZnO. We find that different methods lead to a consensus conclusion; that is, although ZnO is interestingly on the edge of becoming a HFE, it is not HFE. We further provide a physical origin that explains why ZnO is not yet a HFE and reveal a possible condition under which ZnO may become a HFE.

II. THEORETICAL METHODS

It is not trivial to investigate the hyperferroelectric properties since they require determining the electric polarization, the electronic screening of electric fields, and the LO phonon after the phonon interacts with macroscopic electric fields. To tackle these complex tasks, we use a combination of different computational methods to study the structural properties, electric polarization, dielectric susceptibility, and lattice vibrations of ZnO, all of which are needed in order to understand the hyperferroelectric properties of ZnO. These techniques are described below.

Total-energy calculations and structure optimization. The density functional theory (DFT) within the local-density approximation [24,25], as implemented in QUANTUM ESPRESSO [26,27], is used to determine the total energy, atomic forces, and optimized structure. Norm-conserving pseudopotentials of Troullier-Martins type are used to mimic the effects of core electrons [28]. Semicore states of Zn $3s$ and $3p$ are treated as the valence states to ensure better accuracy, and details of the atomic pseudopotentials were given in Ref. [16]. These pseudopotentials have been successfully used to determine the electromechanical d_{33} coefficient in ZnO under finite electric fields [16] and to predict an interesting phase transition when ZnO is subjected to in-plane tensile strains [29].

Modern theory of polarization. Electric polarization in a solid consists of contributions from both ions and electrons. The ionic contribution $\vec{P}_{\rm ion}$ can be calculated straightforwardly using point charges. The electronic contribution $\vec{P}_{\rm el}$ is determined using the geometrical Berry-phase approach according to the modern theory of polarization [30,31]. More specifically, given Bloch wave functions $|u_{n\vec{k}}\rangle$ at wave vector $\vec{k}$, $\vec{P}_{\rm el}$ is calculated as $\vec{P}_{\rm el}=i\frac{2e}{(2\pi)^3}\int d\vec{k}\langle u_{n\vec{k}}|\nabla_{\vec{k}}|u_{n\vec{k}}\rangle=\frac{2e}{(2\pi)^3}\int d\vec{k}_\perp\phi(\vec{k}_\perp)$, and the polarization contribution $\phi(\vec{k}_\perp)$ at each $\vec{k}_\perp$ is [30,31]

$$\phi(\vec{k}_\perp)=i\sum_{n=1}^{M}\int d\vec{k}_\parallel\langle u_{n\vec{k}}|\frac{\partial}{\partial k_\parallel}|u_{n\vec{k}}\rangle = {\rm Im}\left\{\ln\prod_j \det(\langle u_{n'\vec{k}_\parallel^j}|u_{n\vec{k}_\parallel^{j+1}}\rangle)\right\}, \quad (1)$$

where $\parallel$ and $\perp$ mean, respectively, parallel and perpendicular to the direction of polarization and M is the number of the occupied bands of an insulator. The electronic polarization $\vec{P}_{\rm el}$ can be further analyzed using the theory of polarization structure, which describes the relationship between the phase $\phi(\vec{k}_\perp)$ and wave vector $\vec{k}_\perp$ [32].

Density functional linear response theory. The density functional perturbation theory (DFPT) [33–35] is used to determine the effective charges, high-frequency dielectric constant ϵ_∞ (namely, the electronic contribution to the dielectric constant), phonon frequencies, and eigenvectors of both noncentrosymmetric and centrosymmetric ZnO. In DFPT theory, the response $|\Delta\psi_n\rangle$ of the electron state to the potential deformation $\Delta V(\vec{r})$ of bare ions caused by atomic vibration is determined by solving the Sternheimer equation [33],

$$(H_{scf}-\varepsilon_n)|\Delta\psi_n\rangle=-(\Delta V_{scf}-\Delta\varepsilon_n)|\psi_n\rangle. \quad (2)$$

To determine whether ZnO retains its polar nature under OCBC with vanishing electric displacement ($\vec{D}=0$), we need to determine the LO-phonon frequency and the structural instability of centrosymmetric ZnO at the Brillouin-zone center. For long-wavelength phonons with a wave vector $\vec{q}$ approaching zero, the interatomic force-constant matrix can be separated into analytic and nonanalytic parts, $C_{ij}^{\alpha\beta}=C_{ij}^{a,\alpha\beta}+C_{ij}^{na,\alpha\beta}$, where i and j are atomic indices and α and β are direction indices. The analytic part $C_{ij}^{a,\alpha\beta}$ is computed from the DFPT perturbation theory [33–35], and the nonanalytic part (due to interaction between lattice vibration and macroscopic electric field) is given as [36] $C_{ij}^{na,\alpha\beta}=\frac{4\pi}{\Omega}e^2\frac{(\vec{q}\cdot\mathbf{Z}_i^*)_\alpha(\vec{q}\cdot\mathbf{Z}_j^*)_\beta}{\vec{q}\cdot\boldsymbol{\epsilon}_\infty\cdot\vec{q}}$, where $\mathbf{Z}_i^*$ is the Born effective-charge tensor of atom i. Since C^{na} is not diagonal, it often causes a strong mixing among different modes. This nonanalytic contribution leads to the difference in frequency between a LO phonon and a TO phonon. A rigorous definition of LO/TO splitting was given in Ref. [37].

III. RESULTS AND DISCUSSION

A. Ground-state properties of polar ZnO

We first describe our first-principles results for the ground-state properties of the noncentrosymmetric (polar) ZnO since polar ZnO is an important semiconductor of technological applications and its properties are of interest to many readers. Ground-state ZnO crystalizes in the wurtzite structure with lattice vectors $\vec{a}_1=a(\frac{1}{2}\vec{i}+\frac{\sqrt{3}}{2}\vec{j})$, $\vec{a}_2=a(-\frac{1}{2}\vec{i}+\frac{\sqrt{3}}{2}\vec{j})$, and $\vec{a}_3=c\vec{k}$, where a is the in-plane lattice constant and c is the out-of-plane lattice constant. Atoms inside a unit cell are shown in Fig. 1, where four nonequivalent atoms are located at $0\vec{a}_1+0\vec{a}_2+0\vec{a}_3$ (Zn1), $0\vec{a}_1+0\vec{a}_2+u\vec{a}_3$ (O1), $\frac{1}{3}\vec{a}_1+\frac{1}{3}\vec{a}_2+\frac{1}{2}\vec{a}_3$ (Zn2), and $\frac{1}{3}\vec{a}_1+\frac{1}{3}\vec{a}_2+(\frac{1}{2}+u)\vec{a}_3$ (O2).

We optimize both cell parameters (a and c/a) and atomic positions (i.e., the internal parameter u), and the optimal values of these quantities are given in Table I. After determining the optimized structure, we then compute, from DFPT linear response calculations, the dielectric components ϵ_∞^{11} and ϵ_∞^{33} of high-frequency dielectric constant and the Born effective charge Z_{33}^* of Zn and O atoms; the results are also shown in Table I.

Our theoretical values of $a=3.250$ Å and $u=0.3791$ in Table I are in good agreement with the experimental mea-

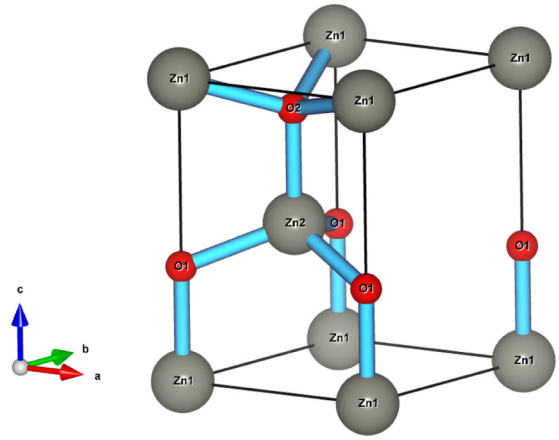

FIG. 1. One unit cell of the wurtzite ZnO crystal, where nonequivalent atoms are labeled as Zn1, Zn2, O1, and O2. The $\vec{a}_1$, $\vec{a}_2$, and $\vec{a}_3$ lattice vectors point at the $\vec{a}$, $\vec{b}$, and $\vec{c}$ directions.

surement results of $a = 3.253$ Å and $u = 0.382$, respectively [38]. The Born effective charge $Z^*_{33} = 2.20$ of Zn in this study is also close to the experimental value [39] of 2.10 and another theoretical value [40] of 2.05. These indicate that our theoretical results are reasonably reliable.

According to the group theory [41], the normal modes at the zone center of polar ZnO (with a wurtzite crystal structure and a point-group symmetry of C_{6v}) are $2A_1 \bigoplus 2B_1 \bigoplus 2E_1 \bigoplus 2E_2$. Among them, A_1(TO) and E_1(TO) are polar modes, B_1 is silent (i.e., both IR and Raman inactive), and E_2 is nonpolar and IR inactive (but Raman active). At the zone center, the acoustic A_1 and E_1 modes are trivial with zero frequencies and are thus not discussed further. For other nontrivial modes in polar ZnO, the computed phonon frequencies ω, IR intensity, and phonon displacements $|d\rangle$ are given in Table II. Phonon displacement $|d\rangle$ is related to the phonon eigenvector $|e\rangle$ by $d_{i\alpha}(l) = \frac{1}{\sqrt{M_i}} e_{i\alpha} e^{i\vec{q}\cdot\vec{R}_l}$, where l, i, and α are, respectively, the indices for lattice sites, atoms inside a cell, and the Cartesian vibration directions and $\vec{q}$ is the phonon wave vector.

The theoretical phonon frequencies are comparable to the experimental measurements [42]. For instance, in Table II, the computed frequencies for A_1(TO) (394 cm^{-1}) and for E_1(TO) (414 cm^{-1}) are in good agreement with the experimental

TABLE I. Theoretical quantities (the second column) obtained from our first-principles calculations for ground-state polar ZnO. The available experimental results are given in the third column for comparison.

Quantities	Present work	Experiments
a (Å)	3.250	3.253 [38]
c/a	1.613	1.603 [39]
u	0.3791	0.382 [38]
ϵ^{11}_{∞}	4.73	
ϵ^{33}_{∞}	5.09	
Z^*_{33} (Zn)	2.20	2.10 [39]
Z^*_{33} (O)	− 2.20	− 2.10

TABLE II. DFPT-calculated phonon frequencies (second column), IR intensity (third column), and phonon displacements (fourth column) of polar ZnO at the zone center. The experimental results on phonon frequencies are given in the parentheses in the second column for comparison [42]. In the fourth column, the vibration direction, i.e., the polarization direction of the phonon, is given as the subscript, and the four components in $|d\rangle$ correspond to the displacements of the Zn1, O1, Zn2, and O2 atoms in sequence.

Phonon	ω (cm^{-1})	IR	Displacement $\|d\rangle$
E_2	86	0.0	$(-0.536, 0.461, 0.536, -0.461)_x$
B_1	258	0.0	$(-0.677, -0.204, 0.677, 0.204)_z$
A_1(TO)	394 (380)	17.3	$(0.169, -0.687, 0.168, -0.686)_z$
E_1(TO)	414 (410)	15.8	$(-0.168, 0.687, -0.168, 0.687)_x$
E_2	445 (438)	0.0	$(-0.146, -0.692, 0.146, 0.692)_x$
B_1	547	0.0	$(0.052, -0.705, -0.052, 0.705)_z$
A_1(LO)	554	17.3	$(-0.168, 0.687, -0.168, 0.687)_z$
E_1(LO)	566	15.8	$(-0.168, 0.687, -0.168, 0.687)_x$

values, which are 380 cm^{-1} for A_1(TO) and 410 cm^{-1} for E_1(TO) [42]. Furthermore, two notable observations can be seen in Table II: (i) The low-frequency phonons, e.g., E_2 at 86 cm^{-1} and B_1 at 258 cm^{-1}, have large contributions from Zn1 and Zn2 cation atoms, while the high-frequency phonons, e.g., A_1(TO) and E_1(TO), have large contributions from O1 and O2 anion atoms. (ii) E_1(LO) and E_1(TO) have nearly identical phonon displacements in ZnO, showing that the LO and TO modes have one-to-one correspondence. This is markedly different from the LO/TO phonons in ferroelectric perovskites $BaTiO_3$ and $PbTiO_3$; in the latter case it is known that LO and TO phonons do *not* have one-to-one correspondence [43,44], and as a result, a rigorous definition of the LO/TO splitting needs to be carefully formulated [37].

B. Electric equations of state: The E-λ and D-λ relations

To find whether ZnO is HFE, we need to determine whether ZnO can retain ferroelectric polarization with nonzero atomic off-center displacements under the OCBC (i.e., under the condition in which electric displacement $\vec{D}$ vanishes along the polar direction). We therefore intend to determine the electric equation of state, which is the relationship between electric displacement and polarization. We use two atomic configurations: One is the ground-state configuration of polar ZnO where the optimal atomic positions are denoted as $\vec{r}_i^{\,\text{opt}}$, and the other is the centrosymmetric configuration of nonpolar ZnO where atoms are located at high-symmetry nonpolar positions (denoted as $\vec{r}_i^{\,c}$). We then construct the intermediate configurations, controlled by the parameter λ as $\vec{r}_i(\lambda) = \vec{r}_i^{\,c} + \lambda(\vec{r}_i^{\,\text{opt}} - \vec{r}_i^{\,c})$. Each λ yields a different atomic configuration with a different polarization. Obviously, the nonpolar configuration and the optimal polar configuration are just two special cases among all possible $\vec{r}_i(\lambda)$ configurations: The former corresponds to $\lambda = 0$, while the latter corresponds to $\lambda = 1$.

We begin with the free energy $F(\lambda)$ when ZnO is under an electric field E, which is applied along the polar direction.

$F(\lambda)$ is defined as [45]

$$F(\lambda) = U(\lambda) - \Omega(\lambda)\left[P(\lambda)E + \tfrac{1}{2}\epsilon_0\chi_\infty(\lambda)E^2\right], \quad (3)$$

where $U(\lambda)$, $P(\lambda)$, $\chi_\infty(\lambda)$, and $\Omega(\lambda)$ are, respectively, the DFT total energy per unit cell, the electric polarization, the diagonal component χ_∞^{33} of high-frequency dielectric permittivity along the polar direction, and the unit-cell volume of ZnO when the bulk solid is at configuration λ. ϵ_0 is the dielectric constant of free space. Since the electric field is applied along the polar direction of ZnO, the vector signs are dropped in Eq. (3). The method of building free energy has also been used in the interface design for enhanced ferroelectricity [46].

Equation (3) is essentially a second-order Taylor expansion of $F(\lambda)$ as a function of E at the configuration λ, with the expansion coefficients $U(\lambda)$, $P(\lambda)$, and $\chi_\infty(\lambda)$ corresponding to the quantities at zero macroscopic field. Therefore, $U(\lambda)$, $P(\lambda)$, and $\chi_\infty(\lambda)$ need to be computed under the short-circuit boundary condition (SCBC) with $E = 0$. On the other hand, since the macroscopic field E in Eq. (3) may be either zero or nonzero, the free energy $F(\lambda)$ in Eq. (3) can thus describe the situations of either SCBC or OCBC or circumstances other than SCBC or OCBC.

For a given E field, the optimal λ should satisfy $\frac{\partial F}{\partial \lambda} = 0$, namely,

$$\frac{\partial U(\lambda)}{\partial \lambda} - \left[\frac{\partial(\Omega P)}{\partial \lambda}E + \frac{1}{2}\epsilon_0\frac{\partial(\Omega\chi_\infty)}{\partial \lambda}E^2\right] = 0. \quad (4)$$

Here it is worth mentioning that knowing how $U(\lambda)$, $P(\lambda)$, and $\chi_\infty(\lambda)$ depend on λ (which can be computed from the DFT and DFPT calculations), it is straightforward to determine, using Eq. (4), the $E \sim \lambda$ relation. In contrast, it is generally not a good idea to determine the *inverse* $\lambda \sim E$ relation, which actually is not needed. Furthermore, Eq. (4) indicates that the E field is determined only by the derivatives $\frac{\partial U(\lambda)}{\partial \lambda}$, $\frac{\partial(\Omega P)}{\partial \lambda}$, and $\frac{\partial(\Omega\chi_\infty)}{\partial \lambda}$, rather than by the magnitudes of U and P.

To obtain the $D \sim \lambda$ relation, we determine using Eq. (3) the electric polarization as $P_{\rm tot} = -\frac{1}{\Omega}\frac{\partial F}{\partial E} = P(\lambda) + \epsilon_0\chi_\infty(\lambda)E$, where the first term accounts for the fact that the electric field will cause ions to displace and the second term accounts for the fact that the electric field will also polarize the wave functions of valence electrons. The electric displacement D then becomes

$$D = \epsilon_0 E + P_{\rm tot} = \epsilon_0[1 + \chi_\infty(\lambda)]E + P(\lambda). \quad (5)$$

When combined with the $E \sim \lambda$ relation obtained from Eq. (4), Eq. (5) leads to the $D \sim \lambda$ relation. Using this $D \sim \lambda$ relation, one can examine whether the atomic off-center displacement λ vanishes under the OCBC ($D = 0$) to find out whether ZnO is HFE. If polar displacement exists (i.e., $\lambda \neq 0$) when $D = 0$, then the solid is a HFE.

In principle, the free energy in the open-circuit (or short-circuit) boundary condition can be obtained using the fixed-E or fixed-D method [45]. However, the computation will be intensive for the following reasons. (i) The electric field in the fixed-E or fixed-D method couples the single-particle states at different electron wave vectors $\vec{k}$, and the Berry-phase calculation of polarization must be inside the charge self-consistent process (not as a postprocess). Both make the computation time-consuming. (ii) Atomic geometry needs to be optimized for each electric field, which further increases computation. In contrast, the current approach used here has several advantages. First, all calculations are performed at zero macroscopic field using common DFT methods, and the approach can thus be widely applied. Further, the approach offers important physics insight, as demonstrated analytically in this paper. We should also mention that the nonlinear effect is largely included in Eq. (3). Since λ depends implicitly on the E field, as shown in Eq. (4), polarization $P(\lambda)$ and high-frequency dielectric susceptibility $\chi_\infty(\lambda)$ thus also depend on E. Therefore, the coupling term $\Omega(\lambda)[P(\lambda)E + \frac{1}{2}\epsilon_0\chi_\infty(\lambda)E^2]$ in Eq. (3) includes the nonlinear effect.

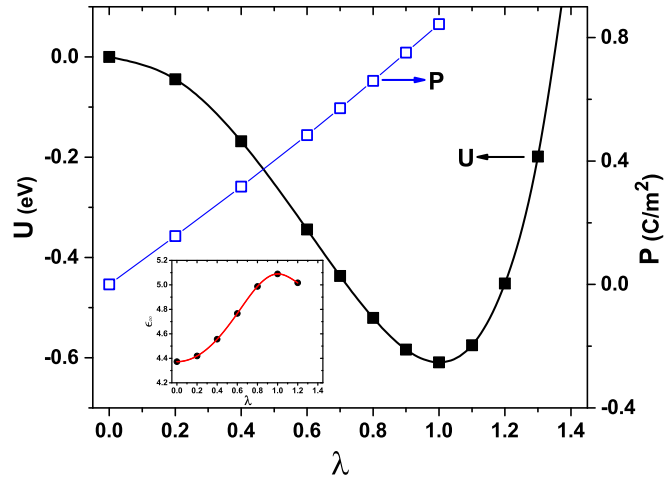

FIG. 2. The total energy U (solid squares, using the left vertical axis) and polarization P (open squares, using the right vertical axis) as a function of λ. The inset shows the high-frequency dielectric constant ϵ_∞ (solid dots) at different λ. These quantities (U, P, and ϵ_∞) are calculated under SCBC. The total energy $U(\lambda = 0)$ at $\lambda = 0$ is chosen to be the zero reference energy. Symbols are the direct DFT calculation results, and lines are fitting curves using cubic splines.

Our calculated $U \sim \lambda$ relation (obtained from DFT structural optimization and total-energy calculations) and the $P \sim \lambda$ relation (obtained from the Berry-phase calculations using the modern theory of polarization) are shown in Fig. 2, while the calculated $\epsilon_\infty \sim \lambda$ relation (obtained from the DFPT linear response calculations) is depicted in the inset of Fig. 2.

From Fig. 2, we see the following: (i) Under the short-circuit boundary condition, the $U \sim \lambda$ curve shows that the nonpolar ZnO (at $\lambda = 0$) is not stable, and polar ZnO (at $\lambda = 1$) is stable, as it should be. When λ is increased to be larger than 1, U increases sharply, which is energetically less favorable. The depth of the potential well $\Delta U = U(\lambda = 1) - U(\lambda = 0)$ is -0.609 eV. This ΔU is, in fact, comparable to the well depths (typically ranging from -0.20 to -0.80 eV) in the recently discovered ABC-type ferroelectrics [47]. (ii) The polarization P depends on λ in a linear fashion, increasing from zero at $\lambda = 0$ to 0.844 C/m^2 at $\lambda = 1$. In other words, $P = 0.844\lambda$, and λ is thus a direct measure of the magnitude of polarization by being proportional to the latter. (iii) High-frequency $\epsilon_\infty(\lambda)$ in the inset of Fig. 2 shows a nonmonotonous dependence on λ, increasing from $\epsilon_\infty = 4.37$ at $\lambda = 0$ to $\epsilon_\infty = 5.09$ at $\lambda = 1$ and then starting to decrease at $\lambda \geqslant 1$.

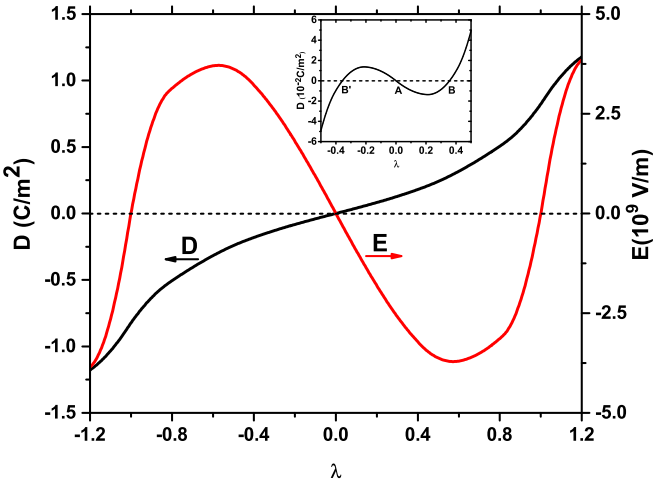

FIG. 3. The $D \sim \lambda$ relation (black curve, using the left vertical axis) and the $E \sim \lambda$ relation (red curve, using the right vertical axis) for ZnO. The inset shows a schematic $D \sim \lambda$ relation which a HFE should exhibit.

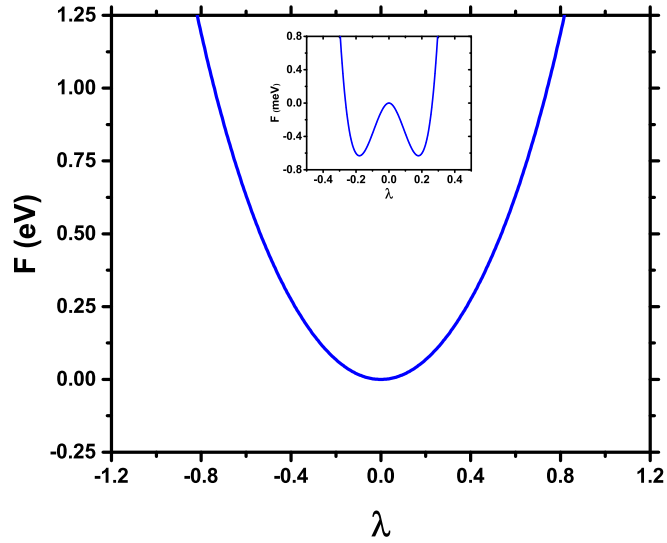

FIG. 4. Free energy $F(\lambda)$ of ZnO under an open-circuit boundary condition as a function of λ. The inset shows the free energy of ZnO under an open-circuit boundary condition when the dielectric constant of centrosymmetric ZnO is increased to $\epsilon_\infty = 10.37$.

The $E \sim \lambda$ relation, determined from Eq. (4), and the $D \sim \lambda$ relation, determined from Eq. (5), are shown in Fig. 3. It is worth pointing out that the $E \sim \lambda$ and $D \sim \lambda$ curves themselves are of considerable significance in terms of understanding the electrical properties, in addition to determining whether a solid is HFE. In fact, electric D displacement was shown to be a fundamental variable in electronic-structure calculations [45,48]. Several marked observations can be made in Fig. 3.

First, interestingly, we see in Fig. 3 that the $E \sim \lambda$ curve has three roots at $\lambda = 0$ and $\lambda = \pm 1$. This does not occur by accident and can be intuitively explained as follows. At the above three λ values, energy U is either a minimum or a saddle point, i.e., $\frac{\partial U(\lambda)}{\partial \lambda} = 0$. Meanwhile, it can be easily seen from Eq. (4) that, when $\frac{\partial U(\lambda)}{\partial \lambda} = 0$, Eq. (4) has a solution of $E = 0$, which explains why $\lambda = 0$ and $\lambda = \pm 1$ must be the roots of the $E \sim \lambda$ curve.

However, the $D \sim \lambda$ curve in Fig. 3 reveals that it has only one root at $\lambda = 0$, showing that only when λ is zero does electric displacement D vanish. Since $\lambda = 0$ corresponds to a nonpolar phase, the $D \sim \lambda$ curve in Fig. 3 thus demonstrates that ZnO is nonpolar under the open-circuit boundary condition $D = 0$, or in other words, ZnO is not HFE. In order to be HFE, the solid needs to exhibit a $D \sim \lambda$ relation, as shown in the inset of Fig. 3, where the curve has three roots at A, B, and B′. At B and B′, λ is nonzero.

It is important to understand why the $D \sim \lambda$ curve of ZnO in Fig. 3 does not possess a nonzero root. We recognize from the $E \sim \lambda$ curve in Fig. 3 that the electric field E at $\lambda = 0.6$ is negative and large in magnitude. Since D is directly related to E, it raises an interesting question, that is, why the D value near $\lambda = 0.6$ is not negative, which may otherwise lead to a nonzero root for D. The question can be answered by Eq. (5). Although the first term in Eq. (5) is negative, the $P(\lambda)$ term at $\lambda = 0.6$ is, nevertheless, positive and dominates, which results in a positive D. We thus see that a large spontaneous polarization could be detrimental to the occurrence of hyperferroelectricity. This result is, interestingly, consistent with the general guideline proposed in Ref. [9] that a HFE needs to have a deep double-potential well and a small polarization.

C. Free energy under the OCBC

An alternative (and efficient) approach to investigate whether a solid is HFE is to determine the free energy under the open-circuit boundary condition. When D vanishes, one obtains, using Eq. (5),

$$E = -\frac{P(\lambda)}{\epsilon_0[1 + \chi_\infty(\lambda)]}. \tag{6}$$

By substituting the above expression into Eq. (3), the free energy F under the $D = 0$ condition can be determined as

$$F(\lambda) = U(\lambda) - \Omega(\lambda)\left\{-\frac{P^2(\lambda)}{\epsilon_0[1 + \chi_\infty(\lambda)} + \frac{1}{2}\chi_\infty(\lambda)\frac{P^2(\lambda)}{\epsilon_0[1 + \chi_\infty(\lambda)]^2}\right\}. \tag{7}$$

One distinctive feature of this free-energy approach is that there is no need to determine the $E \sim \lambda$ and $D \sim \lambda$ relations (which are often less accurate since they require numerical derivatives). Instead, knowing the $U(\lambda)$, $P(\lambda)$, and $\chi_\infty(\lambda)$ curves as computed in Fig. 2, we can directly calculate, using Eq. (7), the free energy as a function of λ.

The free energy for ZnO under OCBC is depicted in Fig. 4. Comparing the $U(\lambda)$ curve in Fig. 2 and the $F(\lambda)$ curve in Fig. 4, we see two critical differences: (i) Although the $U(\lambda)$ curve has a minimum at $\lambda = 1$ (which forms one of the two minima of the double-potential well), the $F(\lambda)$ curve nevertheless has only one minimum at $\lambda = 0$. (ii) U is unstable at $\lambda = 0$ by being a saddle point, but F is stable at $\lambda = 0$. Figure 4 thus reveals that, under the OCBC, the free energy of ZnO is stable only in the *nonpolar* phase with $\lambda = 0$. In other words, ZnO is nonpolar under the OCBC. Therefore,

ZnO is not HFE, which is consistent with the results obtained from the electric equation of state in the previous section.

From the point of view of free energy, the reason that ZnO is not HFE can be understood as follows. Under the OCBC, if ZnO is polar with nonzero polarization, then a nonzero depolarization E field will be generated according to Eq. (6). This strong and nonvanishing depolarization field increases the contribution of the second term in Eq. (7) to the free energy, which ultimately eliminates the polarization.

The theoretical finding that ZnO is not HFE is consistent with available experimental observation. In experiment, the polar surface of ZnO was found to be unstable, and it undergoes surface reconstruction [49]. The observation is in agreement with our result that ZnO is not polar under the OCBC. Furthermore, according to our theory, the instability of the ZnO polar surface is caused by the existence of a strong depolarization field.

D. LO phonon in ZnO

When a hyperferroelectric solid is in its (unstable) centrosymmetric phase, its *longitudinal*-optic (LO) phonon should exhibit an imaginary frequency at the zone center [1,9,10], which manifests the fact that ferroelectric instability persists despite the existence of a depolarizing field. Here it is worth pointing out that, when a solid is in the centrosymmetric phase, whereas a soft *transverse*-optic (TO) phonon at the zone center is quite common and indicates the existence of ferroelectric instability [7], a soft LO phonon at the zone center is rare, which explains why a HFE is unique and special.

To determine whether ZnO possesses a soft LO phonon, we have computed the TO and LO frequencies of the centrosymmetric (nonpolar) ZnO, using the DFPT linear response theory. We find $\omega_{\mathrm{TO}} = 243i$ cm^{-1}, showing that nonpolar ZnO is unstable with an imaginary ω_{TO} frequency under the short-circuit boundary condition of $E = 0$, as it should be. Meanwhile, we find $\omega_{\mathrm{LO}} = 255$cm^{-1}, revealing that nonpolar ZnO is stable with a large and positive ω_{LO} frequency under the open-circuit boundary condition of $D = 0$. This reveals that ZnO is not HFE.

It is interesting to go one step further and explore why ZnO is not HFE, although it has a wurtzite structure similar to the ABC-type semiconductor LiZnAs; LiZnAs, on the other hand, was discovered to be HFE [1]. We find that the difference may be attributed to the small high-frequency dielectric constant ϵ_∞ in ZnO. To demonstrate this, we examine nonpolar ZnO and numerically change its ϵ_∞ value and then compute the nonanalytic part $C_{ij}^{na,\alpha\beta}$ of the dynamical matrix as well as the frequency of the LO phonon. The obtained frequency squared ω_{LO}^2 of the LO phonon is shown in Fig. 5 as a function of ϵ_∞. The DFT-computed value of ϵ_∞ is 4.37 for nonpolar ZnO. Figure 5 shows that, when ϵ_∞ is artificially increased from 4.37, ω_{LO}^2 decreases sharply. As ϵ_∞ is increased to a critical value $\epsilon_\infty^c = 9.12$, ω_{LO}^2 becomes negative, and ZnO becomes a HFE. The result reveals that a moderate increase in ϵ_∞ will turn ZnO into a HFE, signaling that a small ϵ_∞ value is indeed responsible for ZnO being non-HFE. Interestingly, this discovery is consistent with LiZnAs and other ABC-type HFE semiconductors, which all have a fairly large ϵ_∞ on the order of $\sim$15 [1].

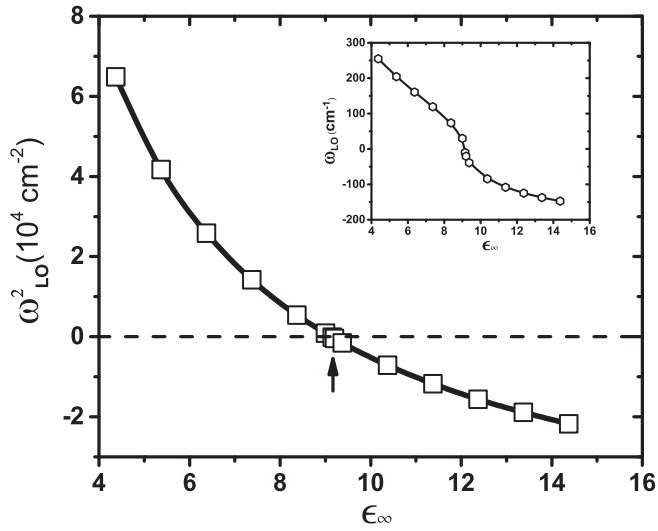

FIG. 5. Frequency squared ω_{LO}^2 of the LO phonon in centrosymmetric ZnO as a function of ϵ_∞. The arrow marks the critical ϵ_∞^c value at which ω_{LO}^2 becomes negative. The inset shows how the LO frequency ω_{LO} varies with ϵ_∞. In the inset, imaginary frequencies are plotted as negative values.

To further confirm that a larger ϵ_∞ value will indeed turn ZnO into a HFE, we change the ϵ_∞ value of nonpolar ZnO to 10.37 (which is larger than the critical value of $\epsilon_\infty^c = 9.12$) and calculate, using Eq. (7), the free energy under the OCBC as a function of λ. The result is depicted in the inset of Fig. 4, showing that the free energy now exhibits *double* minima at nonzero $\lambda = \pm 0.18$. Therefore, ZnO indeed becomes a HFE when ϵ_∞ is increased. The fact that ZnO can be turned into a HFE also suggests that, compared to LiZnAs, wurtzite semiconductors may become hyperferroelectric without Li.

There are two possible routes in experiments to change the ϵ_∞ value in ZnO. One is by biaxial in-plane strain [29], and the other is by doping. Both routes will alter the band gap of ZnO and thus the high-frequency electronic contribution to the dielectric constant.

Our theoretical study also provides a unified scheme linking different explanations for the origin of hyperferroelectricity [1,9–11]. From the point of view of a LO phonon, a large high-frequency dielectric ϵ_∞ constant will reduce the LO/TO splitting and give rise to a soft LO phonon, which is consistent with the explanation of Garrity *et al.* that a HFE is caused by small LO/TO splitting [1] . Meanwhile, a large ϵ_∞ constant will also lead to metascreening, which is in agreement with the explanation in Ref. [11]. From the point of view of the free energy under the OCBC, a small spontaneous polarization, a large high-frequency dielectric χ_∞ susceptibility, and a deep potential well all favor the emergence of double minima in free energy [see Eq. (7)], which is consistent with the explanation of Ref. [9]. Furthermore, a large dielectric ϵ_∞ constant will lead to a strong screening of the long-range interaction and make the short-range interaction become prominent in causing hyperferroelectricity, which is in line with the explanation in Ref. [10].

To confirm that our theory in Eq. (7) also works for other materials, we apply it to LiBeSb, one of the hyperferroelectrics in Ref. [1]. As shown in the inset of Fig. 4, in order for a solid to be hyperferroelectric, the free energy F in Eq. (7) should have double minima. In other words, the $F \sim \lambda$ curve should have a *negative* curvature near $\lambda = 0$. By using the computation data available in Ref. [1], we find that the $F \sim \lambda$ relation for LiBeSb is $F = -0.1686\lambda^2$ eV per unit cell, showing that the curvature is, indeed, negative. Therefore, LiBeSb is a hyperferroelectric according to Eq. (7), and our theory is thus general and works for other materials.

IV. SUMMARY

Hyperferroelectricity is an interesting phenomenon, and understanding whether a solid is HFE is a topic of importance. We have described three approaches to investigate the hyperferroelectric properties of ZnO, which include (a) determining the electric equation of state, (b) calculating the free energy under OCBC, and (c) determining the properties of a LO phonon. The current study also provides a unified scheme linking different explanations for the origin of hyperferroelectricity. Our specific findings are summarized in the following.

(i) The $E \sim \lambda$ relation was shown to be determined only by the derivatives $\frac{\partial U(\lambda)}{\partial \lambda}$, $\frac{\partial(\Omega P)}{\partial \lambda}$, and $\frac{\partial(\Omega \chi_\infty)}{\partial \lambda}$, as revealed in Eq. (4). For a ferroelectric solid, we found that the $E \sim \lambda$ curve must have three roots at $\lambda = 0$ and $\lambda = \pm 1$.

When ZnO is under the *short-circuit* boundary condition, the depth ΔU of the double-potential well is found to be 0.609 eV, which is comparable to those in ABC-type semiconductor ferroelectrics [47]. The polarization in ZnO was shown to be directly proportional to λ as $P = 0.844\lambda$ C/m^2.

On the other hand, when ZnO is under the *open-circuit* boundary condition, we found that its $D \sim \lambda$ curve exhibits only one root at $\lambda = 0$, showing that ZnO possesses no polarization when $D = 0$. ZnO is thus not a HFE. The absence of a nonzero root in the $D \sim \lambda$ curve of ZnO can be attributed to the large spontaneous polarization; namely, the second term in Eq. (5) is detrimentally too large.

(ii) To predict whether a solid is HFE, we found that an alternative (and more effective) approach is to calculate, directly using Eq. (7), the free energy under the OCBC, which bypasses the determination of the $D \sim \lambda$ relation. Using this approach, we revealed that the free energy of ZnO under the OCBC is most stable at $\lambda = 0$, and ZnO is thus not polar under the OCBC, which is consistent with the result obtained from the electric equation of state.

(iii) For centrosymmetric ZnO, our linear response calculations yielded a soft TO mode with frequency $\omega_{\mathrm{TO}} = 243i\ \mathrm{cm}^{-1}$, which shows that ZnO has a polar instability under the short-circuit boundary condition. But the LO frequency $\omega_{\mathrm{LO}} = 255\ \mathrm{cm}^{-1}$ does not have an imaginary frequency and is not soft, revealing that ZnO is stable (and thus not a HFE) under the open-circuit boundary condition.

Furthermore, the fact that ZnO is not a HFE originates from its small high-frequency dielectric constant. We showed that, when ϵ_∞ of ZnO is increased beyond a critical value $\epsilon_\infty^c = 9.12$, ZnO indeed becomes a HFE by possessing a soft LO mode (as shown in Fig. 5) as well as double minima of the free energy (as depicted in the inset of Fig. 4).

Considering that hyperferroelectricity is still at the beginning and remains not adequately understood, we hope that our study will stimulate more theoretical and experimental work on this interesting phenomenon.

ACKNOWLEDGMENTS

This work was partially supported by the Office of Naval Research. Computations were performed at the computing facilities provided by the Arkansas High-Performance Computing Center, supported by NSF.

[1] K. F. Garrity, K. M. Rabe, and D. Vanderbilt, Phys. Rev. Lett. **112**, 127601 (2014).
[2] N. A. Benedek and M. Stengel, Physics **7**, 32 (2014).
[3] C. J. Fennie and K. M. Rabe, Phys. Rev. B **72**, 100103 (2005).
[4] E. Bousquet, M. Dawber, N. Stucki, C. Lichtensteiger, P. Hermet, S. Gariglio, J.-M. Triscone, and P. Ghosez, Nature (London) **452**, 732 (2008).
[5] N. A. Benedek and C. J. Fennie, Phys. Rev. Lett. **106**, 107204 (2011).
[6] M. Stengel, C. J. Fennie, and P. Ghosez, Phys. Rev. B **86**, 094112 (2012).
[7] M. E. Lines and A. M. Glass, *Principles and Applications of Ferroelectrics and Related Materials* (Clarendon, Oxford, 1977).
[8] M. Dawber, K. M. Rabe, and J. F. Scott, Rev. Mod. Phys. **77**, 1083 (2005).
[9] H. Fu, J. Appl. Phys. **116**, 164104 (2014).
[10] P. Li, X. Ren, G.-C. Guo, and L. He, Sci. Rep. **6**, 34085 (2016).
[11] H. J. Zhao, A. Filippetti, C. Escorihuela-Sayalero, P. Delugas, E. Canadell, L. Bellaiche, V. Fiorentini, and J. Iniguez, Phys. Rev. B **97**, 054107 (2018).
[12] S. Liu and R. E. Cohen, Phys. Rev. Lett. **119**, 207601 (2017).
[13] Z. W. Pan, Z. R. Dai, and Z. L. Wang, Science **291**, 1947 (2001).
[14] P. X. Gao, Y. Ding, W. Mai, W. L. Hughes, C. Lao, and Z. L. Wang, Science **309**, 1700 (2005).
[15] N. A. Hill and U. Waghmare, Phys. Rev. B **62**, 8802 (2000).
[16] D. Karanth and H. Fu, Phys. Rev. B **72**, 064116 (2005).
[17] H. Fu and L. Bellaiche, Phys. Rev. Lett. **91**, 057601 (2003).
[18] S.-E. Park and T. R. Shrout, J. Appl. Phys. **82**, 1804 (1997).
[19] A. Garcia and D. Vanderbilt, Appl. Phys. Lett. **72**, 2981 (1998).
[20] H. Fu and R. E. Cohen, Nature (London) **403**, 281 (2000).
[21] F. A. Ponce and D. P. Bour, Nature (London) **386**, 351 (1997).
[22] C. H. Park, S. B. Zhang, and S.-H. Wei, Phys. Rev. B **66**, 073202 (2002).
[23] S. Limpijumnong, S. B. Zhang, S.-H. Wei, and C. H. Park, Phys. Rev. Lett. **92**, 155504 (2004).
[24] P. Hohenberg and W. Kohn, Phys. Rev. **136**, B864 (1964).
[25] W. Kohn and L. J. Sham, Phys. Rev. **140**, A1133 (1965).
[26] P. Giannozzi *et al.*, J. Phys.: Condens. Matter **21**, 395502 (2009).
[27] QUANTUM ESPRESSO, http://www.quantum-espresso.org.
[28] N. Troullier and J. L. Martins, Phys. Rev. B **43**, 1993 (1991).
[29] Z. Alahmed and H. Fu, Phys. Rev. B **77**, 045213 (2008).

[30] R. D. King-Smith and D. Vanderbilt, Phys. Rev. B **47**, 1651 (1993).
[31] R. Resta, Rev. Mod. Phys. **66**, 899 (1994).
[32] Y. Yao and H. Fu, Phys. Rev. B **79**, 014103 (2009).
[33] S. Baroni, S. de Gironcoli, A. Dal Corso, and P. Giannozzi, Rev. Mod. Phys. **73**, 515 (2001).
[34] S. Baroni, P. Giannozzi, and A. Testa, Phys. Rev. Lett. **58**, 1861 (1987).
[35] X. Gonze, Phys. Rev. A **52**, 1096 (1995).
[36] X. Gonze and C. Lee, Phys. Rev. B **55**, 10355 (1997).
[37] A. Raeliarijaona and H. Fu, Phys. Rev. B **92**, 094303 (2015).
[38] H. Karzel, W. Potzel, M. Kofferlein, W. Schiessl, M. Steiner, U. Hiller, G. M. Kalvius, D. W. Mitchell, T. P. Das, P. Blaha, K. Schwarz, and M. P. Pasternak, Phys. Rev. B **53**, 11425 (1996).
[39] K.-H. Hellwege and O. Madelung, Numerical Data and Functional Relationships in Science and Technology, *Landolt-Bornstein, New Series*, Group III, Vol. 17a (Springer, New York, 1982); Numerical Data and Functional Relationships in Science and Technology, *Landolt-Bornstein, New Series*, Group III, Vol. 22a (Springer, New York, 1982).
[40] A. Dal Corso, M. Posternak, R. Resta, and A. Baldereschi, Phys. Rev. B **50**, 10715 (1994).
[41] M. S. Dresselhaus, G. Dresselhaus, and A. Jorio, *Group Theory* (Springer, Berlin, 2010).
[42] J. Serrano, F. J. Manjon, A. H. Romero, A. Ivanov, M. Cardona, R. Lauck, A. Bosak, and M. Krisch, Phys. Rev. B **81**, 174304 (2010).
[43] W. Zhong, R. D. King-Smith, and D. Vanderbilt, Phys. Rev. Lett. **72**, 3618 (1994).
[44] D. M. Eagles, J. Phys. Chem. Solids **25**, 1243 (1964).
[45] M. Stengel, N. A. Spaldin, and D. Vanderbilt, Nat. Phys. **5**, 304 (2009).
[46] H. Wang, J. Wen, D. J. Miller, Q. Zhou, M. Chen, H. N. Lee, K. M. Rabe, and X. Wu, Phys. Rev. X **6**, 011027 (2016).
[47] J. W. Bennett, K. F. Garrity, K. M. Rabe, and D. Vanderbilt, Phys. Rev. Lett. **109**, 167602 (2012).
[48] M. Stengel, D. Vanderbilt, and N. Spaldin, Nat. Mater. **8**, 392 (2009).
[49] O. Dulub, U. Diebold, and G. Kresse, Phys. Rev. Lett. **90**, 016102 (2003).